RI 9534

REPORT OF INVESTIGATIONS/1995

A Case Study of Shield-Strata Interaction at a Southern Ohio Mine

By David C. Oyler

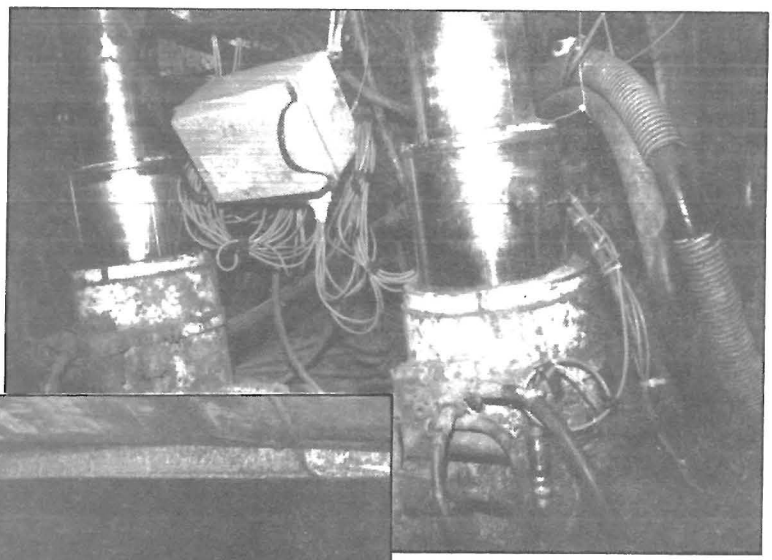

UNITED STATES DEPARTMENT OF THE INTERIOR

BUREAU OF MINES

U.S. Department of the Interior
Mission Statement

As the Nation's principal conservation agency, the Department of the Interior has responsibility for most of our nationally–owned public lands and natural resources. This includes fostering sound use of our land and water resources; protecting our fish, wildlife, and biological diversity; preserving the environmental and cultural values of our national parks and historical places; and providing for the enjoyment of life through outdoor recreation. The Department assesses our energy and mineral resources and works to ensure that their development is in the best interests of all our people by encouraging stewardship and citizen participation in their care. The Department also has a major responsibility for American Indian reservation communities and for people who live in island territories under U.S. administration.

***Cover:** Legs of roof support shields are shown in the top picture. The legs are instrumented with a recorder and a pressure transducer as part of a study on more effective use of this roof support system. The bottom photograph shows the longwall face area at the time the shields were installed.*

Report of Investigations 9534

A Case Study of Shield-Strata Interaction at a Southern Ohio Mine

By David C. Oyler

UNITED STATES DEPARTMENT OF THE INTERIOR
Bruce Babbitt, Secretary

BUREAU OF MINES
Rhea L. Graham, Director

International Standard Serial Number
ISSN 1066-5552

CONTENTS

ILLUSTRATIONS

TABLES

UNIT OF MEASURE ABBREVIATIONS USED IN THIS REPORT

With Factors for Conversion to U.S. Customary Units

To convert from—		To—	Multiply by—
h	hour		
kN	kilonewton	ton-force (short)	0.11240
kPa	kilopascal	pound-force per square inch	0.14503774
kPa/min	kilopascal per minute	pound-force per square inch per minute	0.14503774
m	meter	foot	3.2808399
min	minute		
pct	percent		
s	second		
V	volt		

Reference to specific products does not imply endorsement by the U.S. Bureau of Mines.

A CASE STUDY OF SHIELD-STRATA INTERACTION AT A SOUTHERN OHIO MINE

By David C. Oyler[1]

ABSTRACT

The U.S. Bureau of Mines studied the interaction of longwall shield supports and adjacent strata at the Meigs No. 31 Mine in southeastern Ohio. Twenty-three legs of twenty shields at midface were instrumented with pressure transducers and monitored for 11 weeks. During the project, leg setting pressures were reduced twice to determine the effect of setting pressure on shield-strata interaction. No correlation was observed between setting pressure and leg loading rates. The shield loading profiles were consistent with a model in which the roof consists of two zones, a thin immediate roof loading the shields well below the typical setting force and a main roof zone essentially supported by the coal and gob and loading shields through its convergence. This model was used to develop an equation for estimating average loading rates at the site. The only variable of the equation is time, and the equation consists of an exponential term to account for the immediate roof loading and a linear term to account for main roof loading. The equation gave good correlation with average loading rates, but the variation in loading from cycle to cycle was too great for the equation to give good predictions of individual cycle loading rates.

[1]Mechanical engineer, Pittsburgh Research Center, U.S. Bureau of Mines, Pittsburgh, PA.

INTRODUCTION

Ground control is an essential element in longwall mining. State-of-the-art shields for mine roof support are now designed with load capacities as high as 8,700 kN (*1-2*)[2] and are typically set at 50 to 70 pct of their maximum capacity. Although high-capacity shields provide effective ground control under most conditions, the available shield capacity is not necessarily used effectively, and usually no attempt is made to monitor shield operation or match shield loading and setting force to actual ground control requirements.

This study had two purposes. The first was to gather data for a long-term, multiple-site study of longwall shield and strata interaction being conducted by the U.S. Bureau of Mines (USBM) as part of its mission to increase worker safety and improve efficiency in U.S. coal mines. The database is to be used to investigate the feasibility of developing algorithms to be incorporated into shield control systems to alert miners to abnormal or dangerous shield loading conditions. The second purpose, and the detailed subject of this report, was to investigate the effect of setting pressure on subsequent shield loading rates and on ground control. As part of the study, attempts were made to reduce shield setting pressures, to collect shield pressure data both before and after the setting pressures had been reduced, and to determine the effect of the reduced setting pressures. An additional goal of the study was to determine the optimum setting pressure or pressure range for the panel and to determine its applicability to other panels.

SITE CHARACTERIZATION

The study site was the A-2 longwall panel of the Meigs No. 31 Mine located in Meigs County in southeastern Ohio (figure 1). The mine operates in the Clarion 4-A Coalbed of the Pennsylvanian Allegheny Group. The A-2 panel is 274 by 2,338 m. Instruments were installed when the panel reached the 756-m point on January 21, 1991, and removed in stages in mid-March and early April at 408 and 354 m, respectively (figure 2).

The coalbed at the site averages 1.44 m in thickness, with a mined height of approximately 1.7 m (some floor rock is mined). The coalbed is nearly flat-lying over the site, with a local dip to the south of less than 0.25° over the instrumented portion of the panel. The overburden ranges from 90 to 120 m over the area of interest and is approximately 50 pct sandstone. The immediate floor rock is a claystone ranging from 1.5 to 5 m in thickness. The roof rock consists of a sequence of limestone, shale or claystone, and sandstone, with typical thicknesses of 1.2, 3, and 21 m, respectively. Locally, the limestone and shale may be washed out by sandstone channels, particularly at the northern ends of the panels. This was the case in the study area at the northern end of the A-2 panel (figure 2).

THEORY

The work at the Meigs No. 31 Mine was guided by a theory of shield-strata interaction that assumes that the roof may be divided into two distinct behavioral classes, an immediate roof and a main roof. The "immediate roof" refers to roof rock that requires support from the shield to remain in equilibrium. The "main roof" is defined as that portion of the roof that is converging in response to mining, but is supported by the unmined coal, the gate road pillars, and the gob. This distinction between main and immediate roof is made in terms of the behavior of the roof, not the rock type or thickness of each layer; and a single layer may exhibit both immediate and main roof behavior.

Physically, the roof may be divided into three distinct zones (figure 3). The zone directly above the coalbed is the complete caving zone, which behaves purely as immediate roof. Next is a transition zone, which is typically called the partial caving zone, where some horizontal forces are transmitted such that the strata are capable of at least partially bridging from the coal panel to the gob, so that the full weight of the strata is generally not borne by the shields. This zone, therefore, exhibits both immediate and main roof behavior. Above it is the main roof zone, which does not require shield support, but which converges and which may load the shield through

[2]Italic numbers in parentheses refer to items in the list of references preceding the appendix at the end of this report.

Figure 1

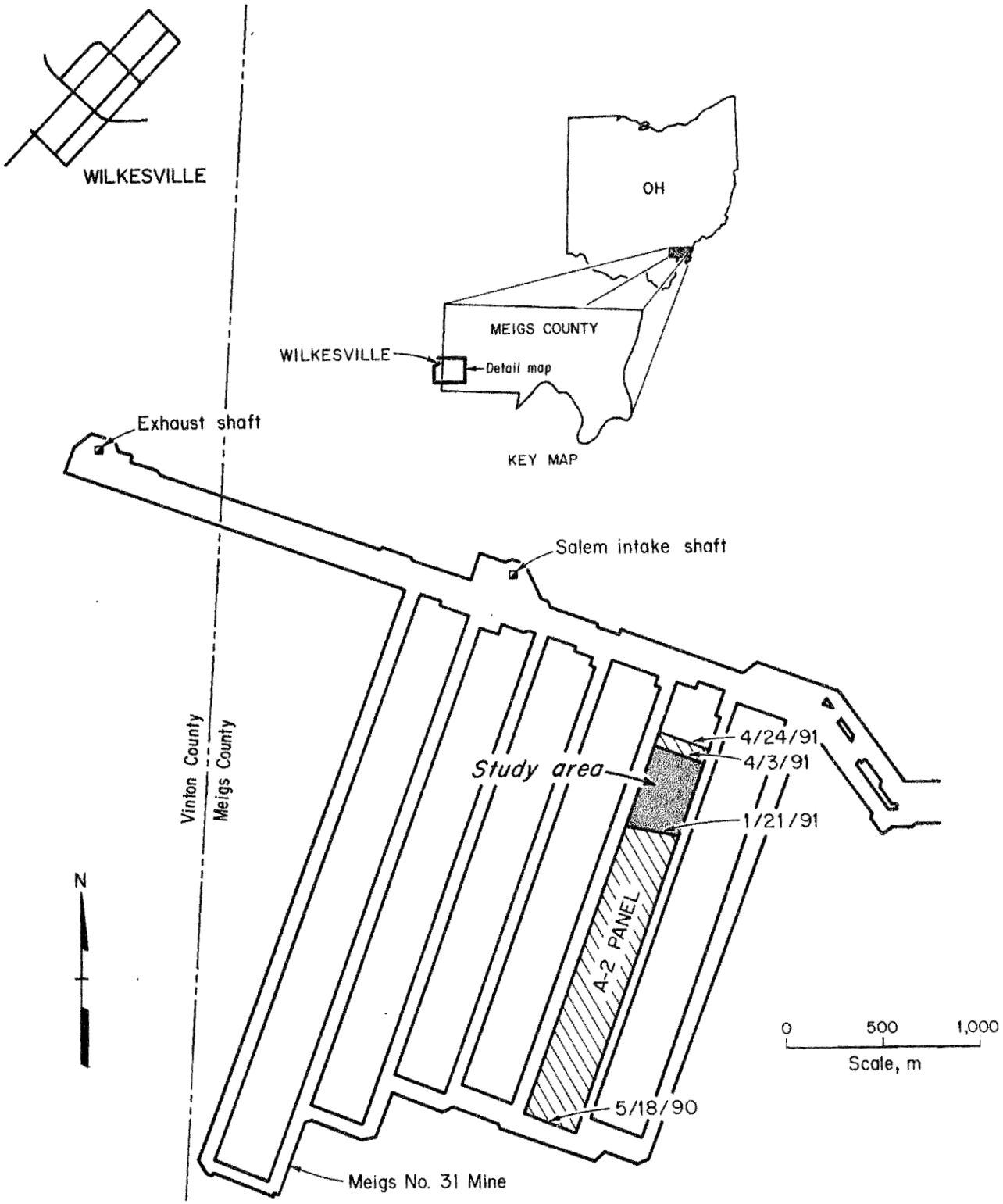

Location of study area.

Figure 2

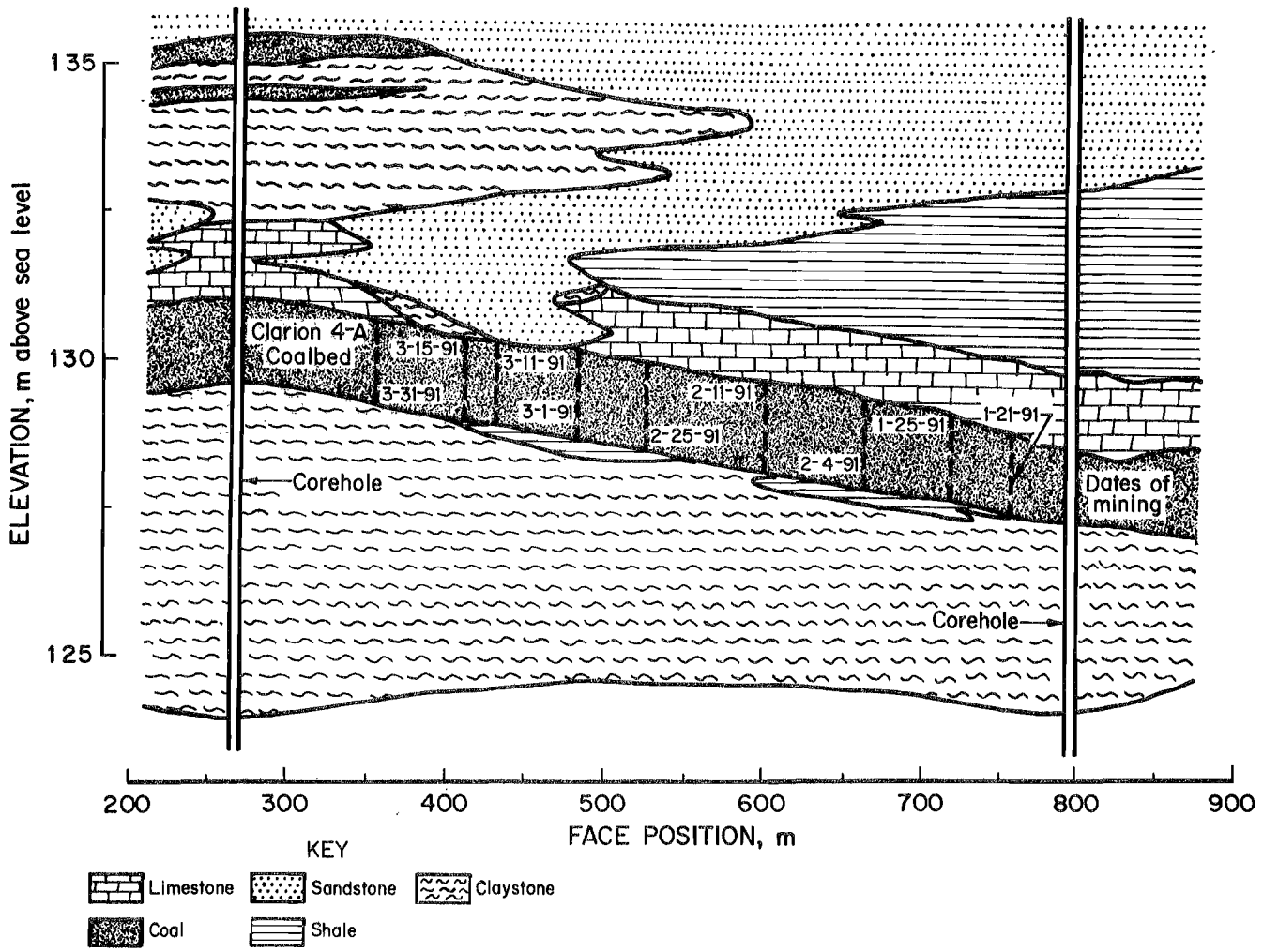

Geologic section of A-2 panel study area, showing progress of mining. Massive sandstone above 135-m elevation is a minimum of 21 m thick.

this convergence. Most classifications of roof behavior recognize only the caving zone and the transition zone, which they refer to as the "immediate roof" and the "main roof" (*3*). In those classification systems, the main roof behavior of rock in or above the transition zone, which converges but is otherwise self supporting, is incorrectly ignored as having no influence upon shield loading.

The working hypotheses in this study are that main roof convergence cannot be significantly retarded by longwall shields and that the roof is sufficiently stable that shields are not necessary to support its weight. The purpose of shields is to maintain the integrity of the immediate roof. Movement of the main roof does cause face convergence and, therefore, loading of the shields. One of the goals of this project is to show that because main roof load is applied to the shields by face convergence and because the stiffness of the shields is essentially constant (that is, the ability of the shields to resist convergence is not affected by preloading), it follows that convergence of the roof and compression of the shield legs will cause shield resistance to be developed. Typical shields will develop their entire load capacity when subjected to a convergence of from 0.01 to 0.04 m (*4*). From ground control considerations alone, it would be possible, in some cases, to use no initial setting pressure at all and rely completely upon passively developed resistance (shield force developed through

compression of the shield legs). In practice, this is not feasible because an initial shield resistance may be required, in some cases, to support the immediate roof and is generally required to provide reaction forces for advancing adjacent shields and the face conveyor.

When the roof requires complete support by the shield, it may be considered as acting as a detached block. In this report, the detached block would be described as exhibiting immediate roof behavior. A detached block should initially load a shield very rapidly, and once the block is fully supported, the loading rate should go to zero (figure 4). The panel A-2 shield-loading curves suggest that the detached block is a relatively uncommon immediate roof condition at the Meigs No. 31 Mine. Only about 5 pct of the shield cycles observed at the Meigs No. 31 Mine gave loading responses that could have been considered to indicate a detached block condition.

More commonly, the roof is partially supported by the coal face and, therefore, acts like a cantilever, or when supported by the gob, forms what might be described as an arch or bridge. It is likely that the most common behavior is a combination of immediate and main roof behaviors. The extreme case of roof fully supported by

Figure 3

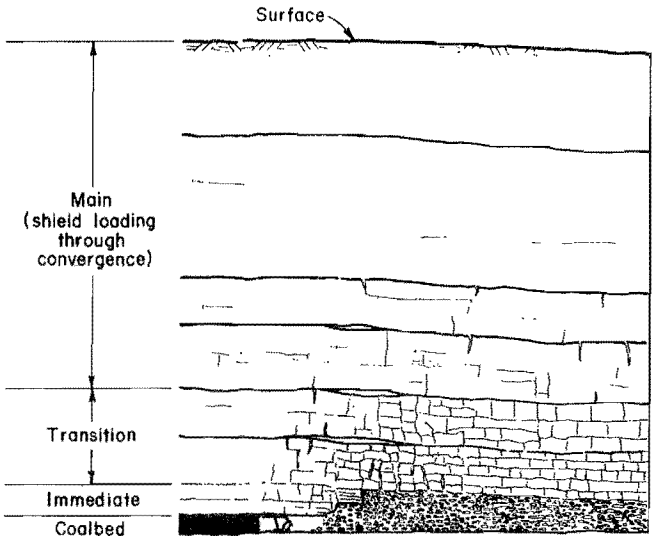

Physical model of shield-strata interaction.

Figure 4

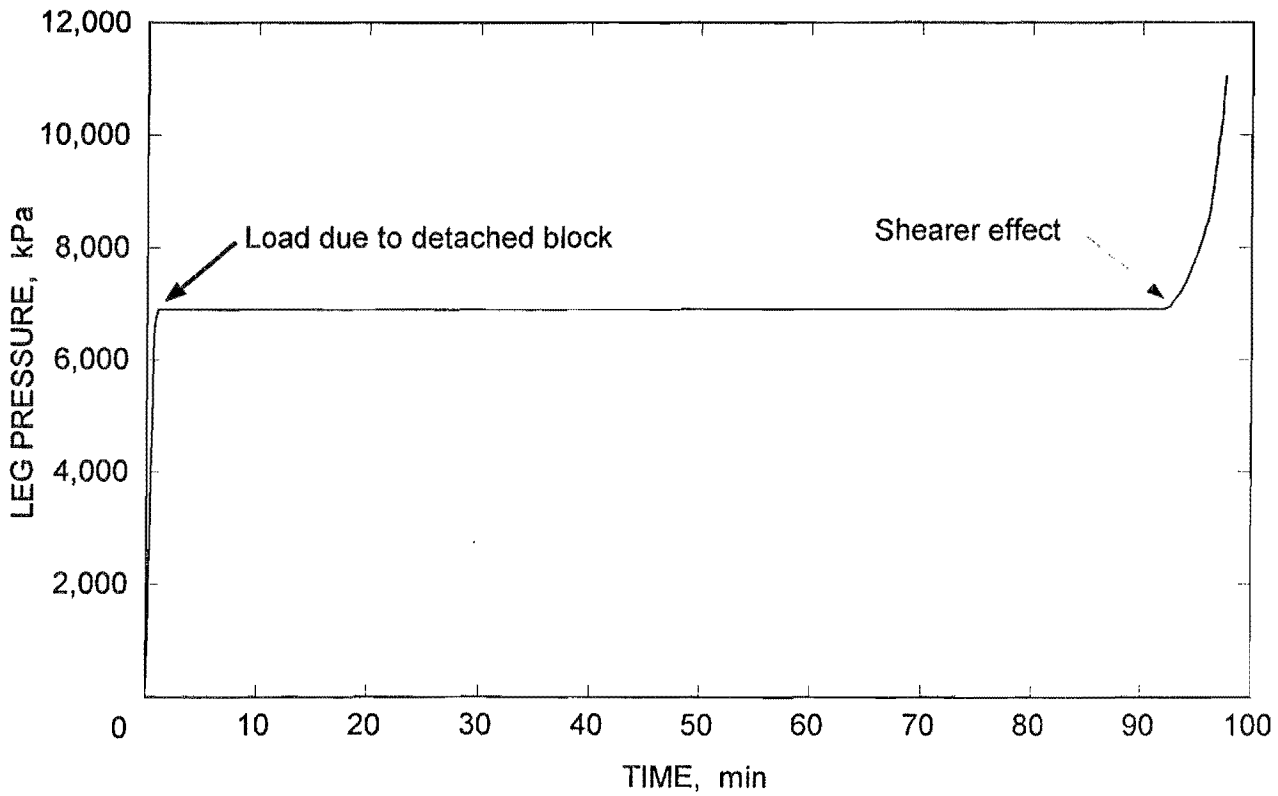

Idealized loading diagram for detached block roof behavior.

the face and gob is essentially the case of main roof loading and is probably also relatively uncommon, except at panel startup before first break. Exclusively main roof loading behavior (figure 5) would be most easily characterized by an absence of the high initial loading rate due to the detached or semidetached roof and by a nearly constant loading rate during the entire shield cycle. However, both detached roof behavior and exclusively main roof behavior are difficult to identify with certainty because of the masking effect of the active pressurization of the shields at the beginning of the cycle. (In this report, the term "cycle" is used to refer both to a single face pass of the shearer and to one pressurization, depressurization, and advance of a shield. In typical operation, the length of a mining cycle and a shield cycle are usually the same, although their start and ending times may be defined differently.) At the end of a shield cycle, the redistribution of load caused by the removal of coal by the shearer causes an increase in shield load just before the shield is lowered and advanced. This shearer effect is also present at the beginning of the cycle, after shield advance, but is obscured by the pressure changes taking place during shield setting.

The thickness of the immediate and main roof layers is difficult to determine since they need not necessarily correspond to particular rock layers. Direct observation of actual roof behavior would be required to determine the height of the immediate and main roof. At the Meigs No. 31 Mine, the geology and underground observation suggest that the immediate roof would be the limestone and the shale or claystone strata. These were approximately 5 m thick on the A-2 panel. The load from a detached block of these rock layers with an effective area equal to the shield canopy area (3.9 by 1.5 m) would have been 780 kN, assuming a rock specific gravity of 2.65. The typical initial setting force on the shields was approximately 2,900 kN, so the shields were typically set to support a detached block of those dimensions up to 18 m high.

Under some conditions, shield force may increase the stiffness and strength of the immediate and transition roof, in much the same way that a roof bolt clamps together rock layers to form a stronger (higher moment of inertia) beam (*5*). Active shield loading is primarily justified under those conditions where the immediate and transition roof may be strengthened by the shield force, causing less roof deflection and leading to an overall reduction in the

Figure 5

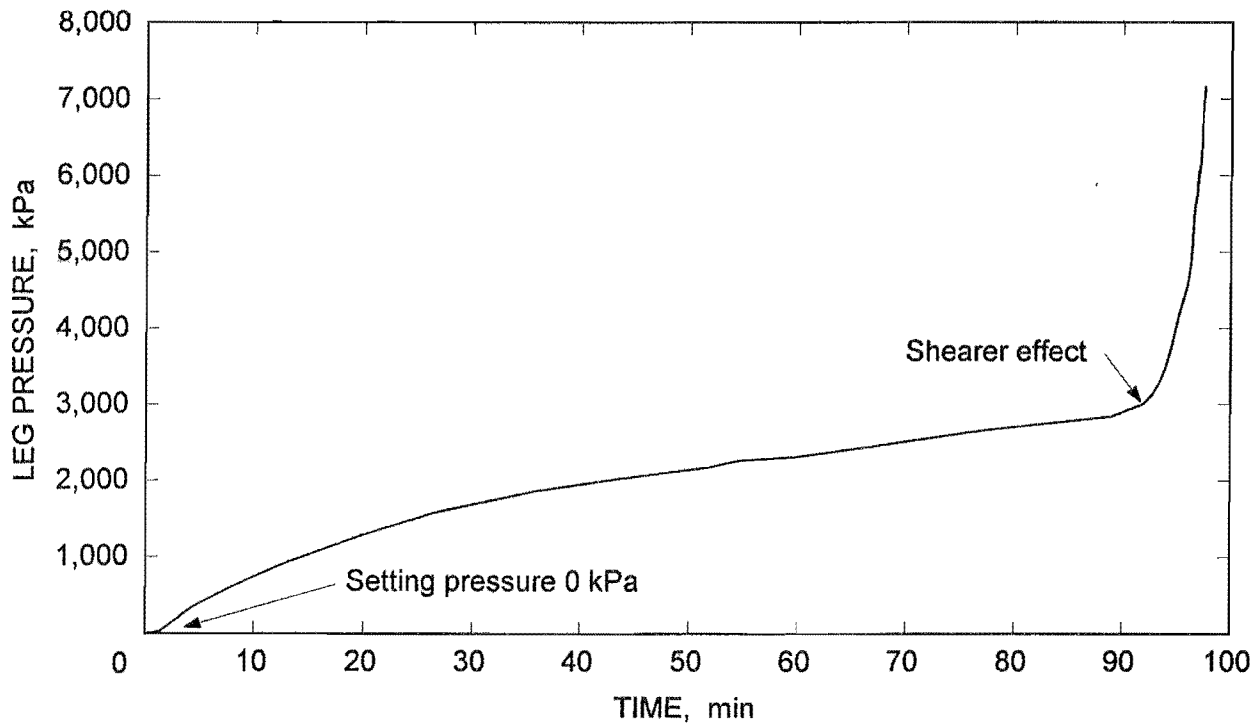

Idealized loading diagram for main roof behavior.

developed shield loading, or where it prevents unacceptable convergence. However, if the load developed through convergence during the cycle is not reduced by more than the required increase in setting pressure, then the total load will actually be higher and an increase in setting pressure will increase the total shield load (figure 6). The data from Meigs No. 31 Mine do not suggest a correlation between setting pressure and maximum pressure and, therefore, suggest that higher setting pressures are unnecessary because they lead to higher average shield pressures, but not improved ground control. Figure 7 shows the loading curves for 21 legs (curves for 2 legs are not shown because one of the legs was leaking and the other had a faulty instrument cable) on the A-2 panel during a typical cycle. Setting pressures ranged from 23,000 to 33,000 kPa during this cycle. Despite the wide variation in setting pressures, there is a striking similarity in the loading rates of almost all legs during the entire cycle. Parallel loading curves, which indicate identical loading rates, are quite common in the A-2 panel data and demonstrate that loading rates are independent of the setting pressure at this site.

INSTRUMENTATION

The instruments installed on the A-2 panel (figure 8) were 24 T-Hydronics TH-M pressure transducers. These transducers have an operating range of 0 to 68,950 kPa and an accuracy of ±0.5 pct of the full-scale reading (±350 kPa); their precision is in the range of ±0.2 pct (±140 kPa). Laboratory dead-weight testing of each transducer confirmed that they met the stated accuracy. One transducer was used to measure hydraulic feed line pressure at the center of the panel (at shield 90), and the remainder of the transducers were installed on 23 legs of shields 81 to 100 inclusive. On shields 82, 90, and 98, both legs were instrumented (figure 9).

The pressure transducers were excited and the output data recorded by a model 21XQM permissible datalogger manufactured by Campbell Scientific, Inc. Three recorders were used on the A-2 face, each capable of handling eight pressure transducers. The datalogger can provide dc excitation voltages of up to 5 V; at Meigs No. 31 Mine the excitation used was 1 V. Pressures were read at intervals of 5 s so that the resetting of shields could be identified and recorded. The datalogger program was written to simultaneously store the pressure readings from all eight channels, contingent upon a pressure change of more than 345 kPa in any one channel. Current pressure measurements were compared with previously stored readings to determine when the 345-kPa change had taken place. During the project, damage to instrument cables caused false triggering of output data, eventually requiring modification of the program to identify and eliminate some of the false triggers. The false triggering sometimes caused the datalogger memory to be filled between the biweekly data collection periods, with the loss of between 1 and 5 days of data, in the worst cases.

SHIELD SETTING PRESSURE

An important part of the Meigs No. 31 Mine study was the plan to reduce setting pressure on shields 86 to 100. Before the project began, the nominal shield setting pressure was 26,000 kPa, about 58 pct of the leg capacity of 45,000 kPa. The plan was to reduce the setting pressure (after a period of baseline data collection), in 5,000-kPa increments, until either the minimum feasible setting pressure was reached or some adverse effect upon roof control was noted. The initial setting pressure change was made on February 5. The second and final one was made on February 21. The nominal setting pressures and the dates they were in effect are shown on table 1. The average setting pressures and standard deviations determined from leg pressure data are also shown in the table. Two sets of pressures are given in the table, one for shields 81 to 85, for which the set pressures were not changed, and a second set for shields 86 to 100, for which the setting pressures were changed. The measured setting pressures were generally higher than the nominal setting pressures, and as the nominal setting pressure was reduced, the disparity between the nominal and the measured average setting pressure increased. A frequency histogram (figure 10) is also presented showing the distribution of setting pressures for 5 weeks of the study period. Figure 10 shows the wide variation to be expected in achieved setting pressures.

Figure 6

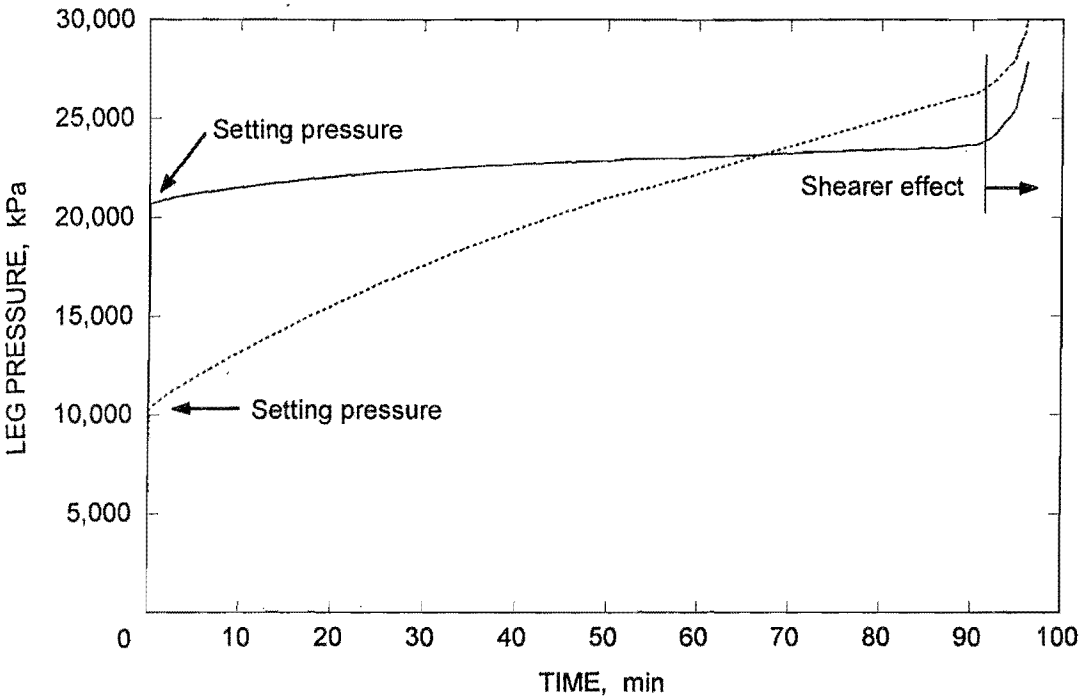

Setting-pressure-sensitive loading curves. This type of loading behavior was not observed at the study site.

Figure 7

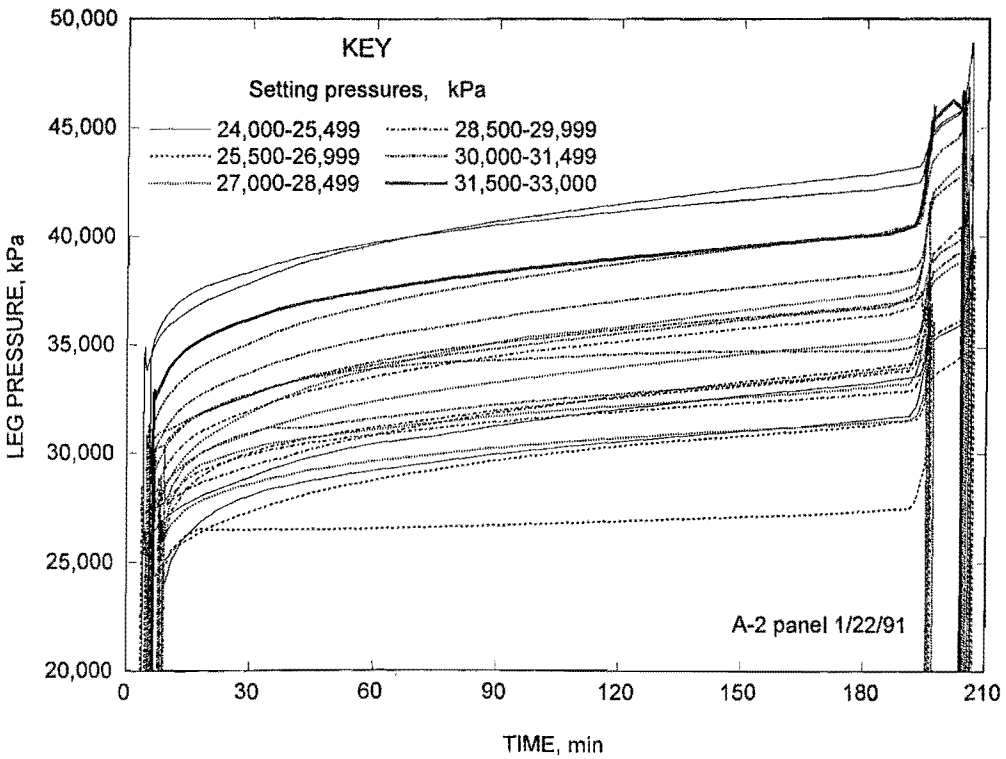

Loading curve for a single shield cycle (1/22/91). Shields 81 to 100.

Figure 8

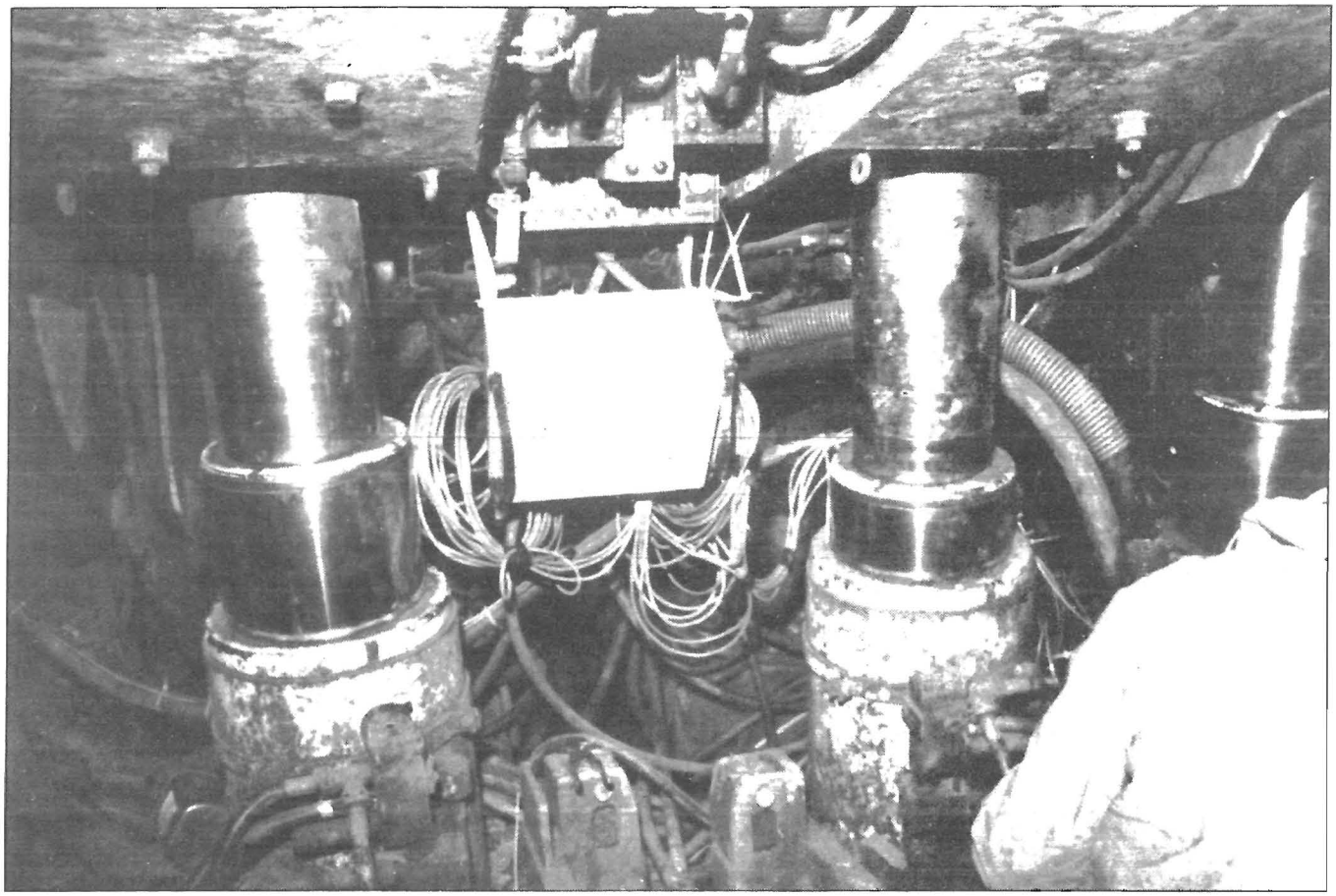

Datalogger station on longwall shield.

Figure 9

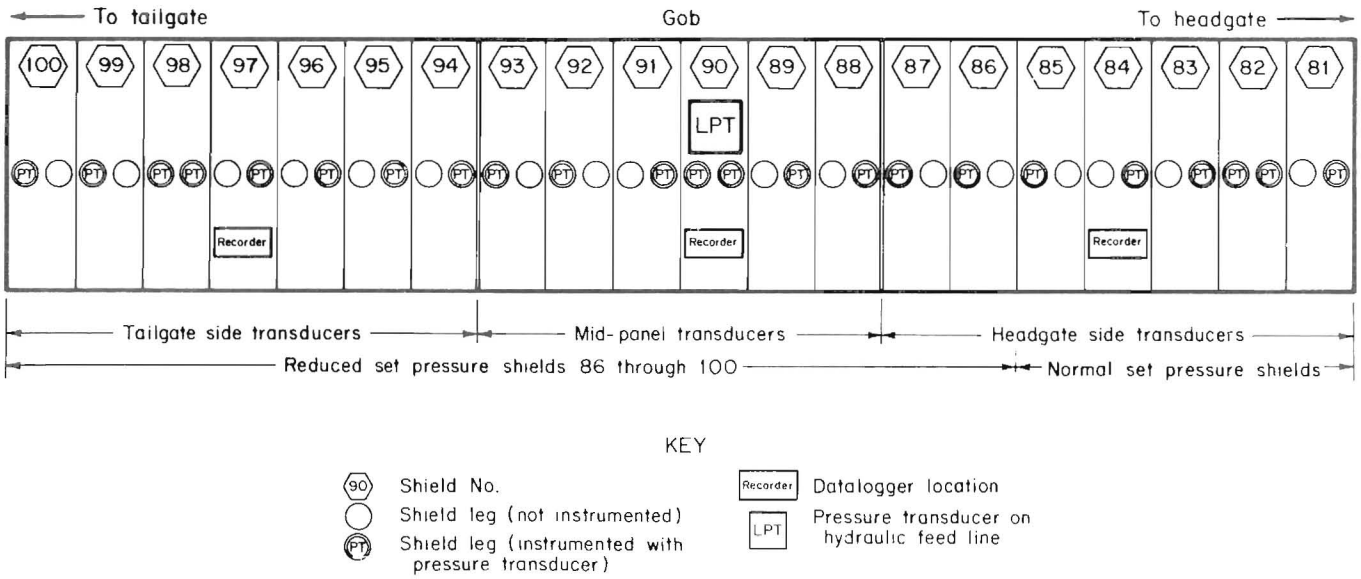

Instrument locations.

Table 1.—Nominal and averaged recorded setting pressures

Dates	Nominal set pressure, kPa		Average set pressure, kPa		Standard deviation, kPa		Number of cycles		Difference, pct	
	H	M&T	H	M&T	H	M&T	H	M&T	H	M&T
1/21 to 1/25	26,000	26,000	26,159	27,055	4,351	4,406	322	812	0.6	4.1
2/04 to 2/05	26,000	26,000	27,090	27,489	3,034	3,041	145	397	4.2	5.8
2/06 to 2/09	26,000	26,000	26,910	25,690	3,234	4,606	417	1,157	3.5	22.4
2/11 to 2/15	26,000	21,000	25,711	25,476	4,371	5,137	303	742	-1.1	21.3
2/25 to 3/01	26,000	17,000	NA	22,732	NA	5,612	NA	911	NA	33.8
3/11 to 3/15	26,000	17,000	24,290	23,842	6,185	6,260	145	546	-6.6	40.3

H Headgate recorder, shields 81 to 85. Set pressure not changed.
M&T Headgate shields 86 and 87. Midpanel and tailgate recorders, shields 86 to 100. Set pressures changed on 2/5 and 2/21.
NA Not available. Insufficient data from shields 81 to 87 for analyses during week of 2/25.

Figure 10

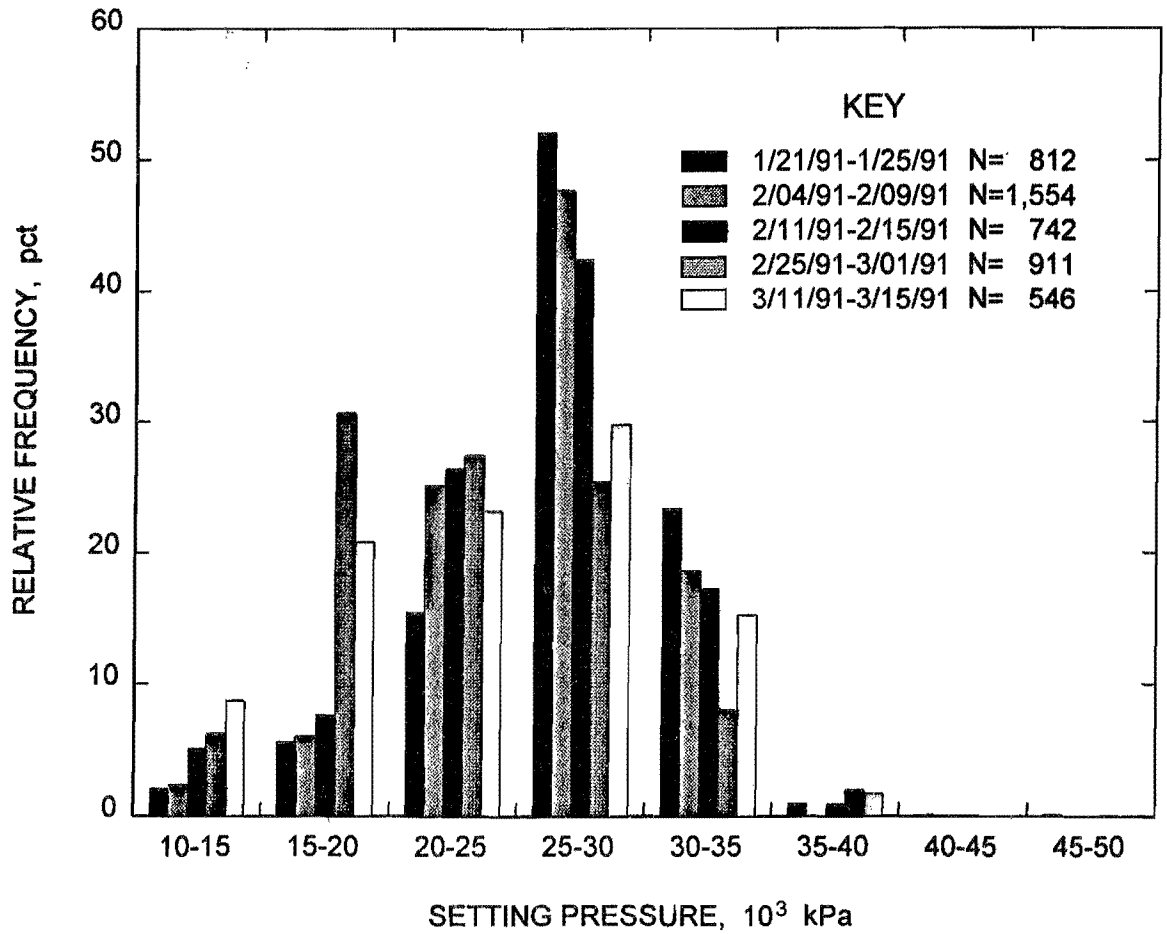

Relative frequency histogram of setting pressures. N = number of cycles.

SET PRESSURE CONTROL

A brief look at the control system of the Westfalia WS 1.7 2X2770 shields (load capacity, 5,540 kN) used on the Meigs No. 31 Mine A-2 panel, explains the difficulties in obtaining the desired setting pressures. Setting pressures measured from other manufacturers' shields indicate that the Westfalia control system is typical of the setting pressure control systems available in the industry today.

The shields on panel A-2 were controlled by a complex logic system that included interlocks against shield lowering until adjacent shields were set and against repressurizing until the shield was advanced. The critical part of the logic sequence from the viewpoint of setting pressure was a test for a pressure known as the transfer pressure, P_1. After advance, and with the leg valves open to the line pressure, the program tested for this pressure (12,000 kPa on the A-2 panel). If P_1 was reached, then other shields were allowed to advance, and a signal was sent to allow an additional time T_5 for the legs to reach setting pressure. If P_1 was not reached, a time T_4 was allowed for the leg to reach P_1 (transfer pressure). If P_1 was not reached after T_4, an error was signaled, but in any case, time T_5 began immediately after T_4. During both time periods, the leg valves remained open to allow hydraulic fluid to enter the legs. At the end of T_5, the program tested for the setting pressure P_2 and shut the leg valve. If the setting pressure was reached, the program stopped; if it was not, an error message was sent and the program then stopped.

The above logic ensures that a shield is given many opportunities to reach setting pressure, but provides limited control over the actual setting pressure. In practice, any setting pressure is possible with this system, although the system is biased in favor of pressures greater than the transfer pressure and pressures close to line pressure. It is not sufficient to change the nominal setting pressure (P_2) to ensure accurate changes in setting pressure in such a system; it is also necessary to adjust the values of P_1, T_4, and T_5, and even then the pressure can either overshoot the setting pressure or never reach it. The large fluctuations found in line pressure (figure 11) on the panel, typically about 7,000 kPa, also increased the uncertainty in the setting pressure.

DISCUSSION

Leg pressure recording instruments were installed at the A-2 panel of the Meigs No. 31 Mine on January 21, 1991. Data were recorded from shields 81 to 100 until March 19, when the recorder for shields 81 to 87 was removed because of cable failures. Additional data were recorded from shields 88 to 100 until April 3, when the remaining two recorders were removed.

Because of the quantity of data available, the data analyzed were limited to those from 5 weeks of the 11-week data collection period: the weeks of January 21, February 4, February 11, February 25, and March 11 (table 1). One-week periods were chosen because studies at other mines have suggested that the weekend shutdown period can have significant effects upon shield-strata interaction and loading rates, and these effects can take several days to disappear (loading rates gradually decline toward zero when the face is idle for periods on the order of a week in length) (*6*). Given similar mining rates, it is possible that leg loading rates will be higher on a Friday than on a Monday. The data were analyzed in 1 week units to eliminate this variable from consideration. The first of the 5 weeks, that of January 21, was chosen as the baseline period, before any attempts were made to change setting pressures. The week of February 4 was a transition period, during which a control system change was made. The week of February 11 shows the effects of the control system change made on February 5 on setting pressures, and the week of February 25 shows the effect on setting pressures of the second control system change, made on February 21. The week of March 11 was chosen so that data from the latter portion of the study could be analyzed.

All of the data collected were corrected for pressure transducer zero, and the times converted from an hour, minute, and second format to a decimal hour format, which made graphing and computation of elapsed time easier. The data were then plotted on graphs of a single day of data for the eight channels from each individual recorder (figure 12). The beginning and end time of each shield cycle was identified through the use of a computer program written for that purpose, and the secant loading rate was determined for each shield leg for each shield cycle. The secant loading rate is easy to calculate and provides a simple characterization of a shield loading cycle. It is determined by dividing the total change in leg pressure during a shield cycle by the duration of the cycle.

The use of secant loading rates can be misleading because of leg yielding. Once a leg reaches its yield pressure, its pressure remains essentially constant, and a continuation of the cycle leads to an apparent reduction in

Figure 11

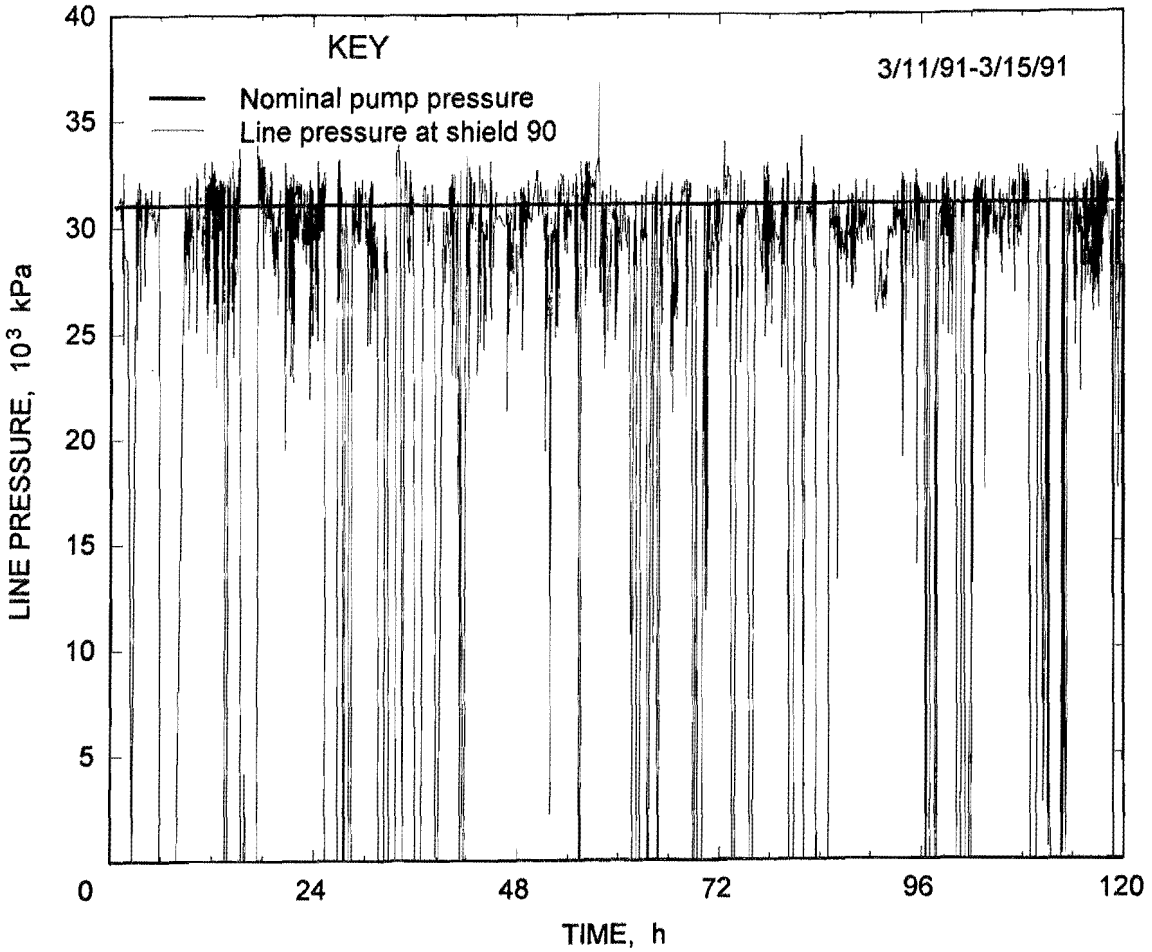

Pressure recorded in main hydraulic line at shield 90.

the secant loading rate. In figure 13, secant loading rates for the period from cycle start to the time of leg yield and from the start to the end of the cycle were compared for cycles grouped into 40-min intervals up to cycle lengths of 480 min. Loading rates to yield were consistently higher, as much as two or three times larger for cycles greater than 120 min in length. The difference is caused primarily by the effect of the leg yield pressure, which places an artificial limit on the maximum pressure change that can occur during any shield cycle. Computing secant loading rates to yield (or to the end of the cycle if yield is not reached) greatly reduces the effect. This procedure was followed to obtain the data used in this report.

Graphs of secant loading rate versus setting pressure were produced for the weeks of January 21, February 4, February 11, February 25, and March 11, for all legs instrumented by each datalogger. A total of five graphs were produced, and these are shown in figure 14. The data shown in these graphs have a wide scatter, and there appears to be no correlation between leg setting pressure and subsequent loading rates. This was the case for all of the 5 weeks studied. A linear regression was then run on each of the data sets. A linear fit was chosen because of its simplicity and because the scatter in the data did not suggest any other model. The least squares fit lines obtained from the linear regressions are shown in figure 14.

Table 2 gives the intercept, slope values, and the squares of the correlation coefficients (r^2) for each linear regression. The r^2 values for the regressions are in the range of 0.0017 to 0.13. The value of r^2 can range from 0 (no correlation) to 1 (a perfect linear correlation). Generally, small r^2 values are unacceptable as an indication

Table 2.—Data from set pressure versus loading rate linear regressions

Data source	Dates	Intercept, kPa	Slope, kPa/min	Number of cycles	Correlation coefficient squared (r^2)
Individual[1]	1/21-1/25	577.355	-0.015119	979	0.0596
	2/04-2/09	581.599	-0.007975	2,029	0.0041
	2/11-2/15	409.715	-0.006610	1,019	0.0255
	2/25-3/01	341.410	-0.005368	896	0.0272
	3/11-3/15	351.398	-0.004865	571	0.0041
Averaged[2]	1/21-1/25	1,866.023	-0.060516	49	0.1042
	2/04-2/09	747.485	-0.010331	92	0.0022
	2/11-2/15	881.736	-0.019875	51	0.0446
	2/25-3/01	483.700	0.001813	66	0.0001
	3/11-3/15	567.498	-0.017102	38	0.0323

[1]Regressions run with the setting pressure and secant loading rate for each leg, for each cycle, were each considered a separate data point. All headgate, midpanel, and tailgate recorder legs were used, except during the week of 2/25 through 3/01/91, when the headgate recorder data were not processed because of the failure of most of the cables leading to that recorder. Negative loading rates, generally indicative of hydraulic fluid leaks, were removed from the individual leg data before the regressions were performed.

[2]All available shield setting pressures and loading rates for each individual cycle were averaged, and a regression was run on the averaged data points. Cycles with fewer than six legs available were not included as points in the averaged data set.

Figure 12

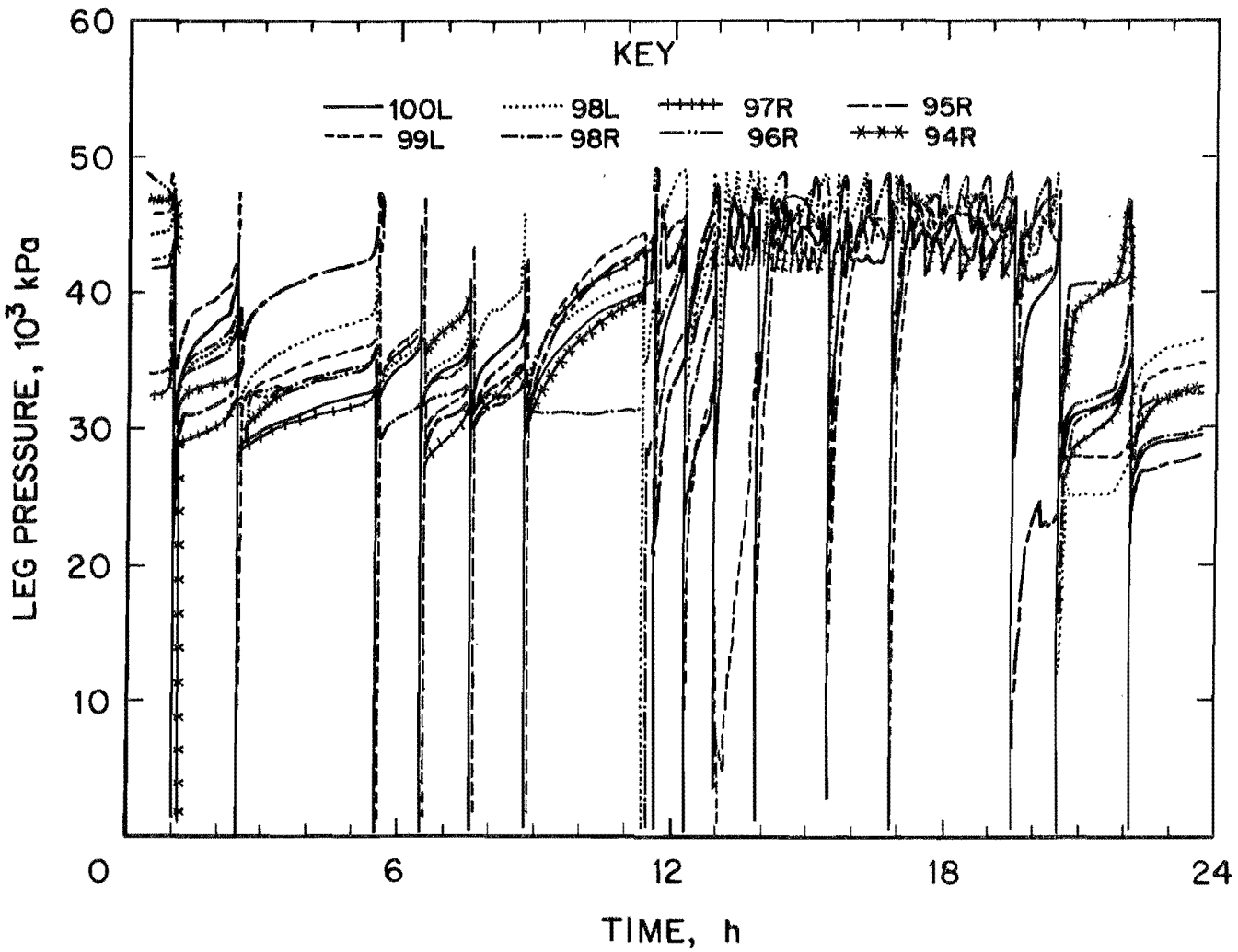

Graph of 1 day of shield pressure data from one datalogger. L = left leg; R = right leg.

of a correlation between two variables. The simplest interpretation of the above data is that there is no correlation between setting pressure and loading rate on A-2 panel at the Meigs No. 31 Mine. If such a correlation exists, it appears to be very weak and has little predictive value. Physically, the assumed mechanism for an effect of shield force on roof loading rates is for shield force to affect the stiffness of the immediate roof. Since the shield force is only one of many factors affecting the immediate roof strength, and since main roof convergence should not be affected by the shield at all, it is to be expected that the correlation between setting pressure and loading rate would be poor. It is more likely that geologic conditions, such as lithology, rock physical properties, and the presence or absence of joints or fractures, have a much greater effect upon roof behavior and, hence, loading rates.

The plots of set pressure versus secant loading rate (figure 14) are for individual shields. It is possible that the reason for the lack of correlation between setting pressure and loading rate is that shields set at low pressure are nonparticipating and the load that they would otherwise be subjected to has been transferred to adjacent shields. This would then tend to decrease the loading rates in shields set at low pressure and increase the loading rates in shields set at high pressure. This hypothesis can be tested in two ways. The simplest is to lower setting pressures across the entire face and compare the loading rates of individual shields from before and after the setting pressure change. A more limited form of this experiment

Figure 13

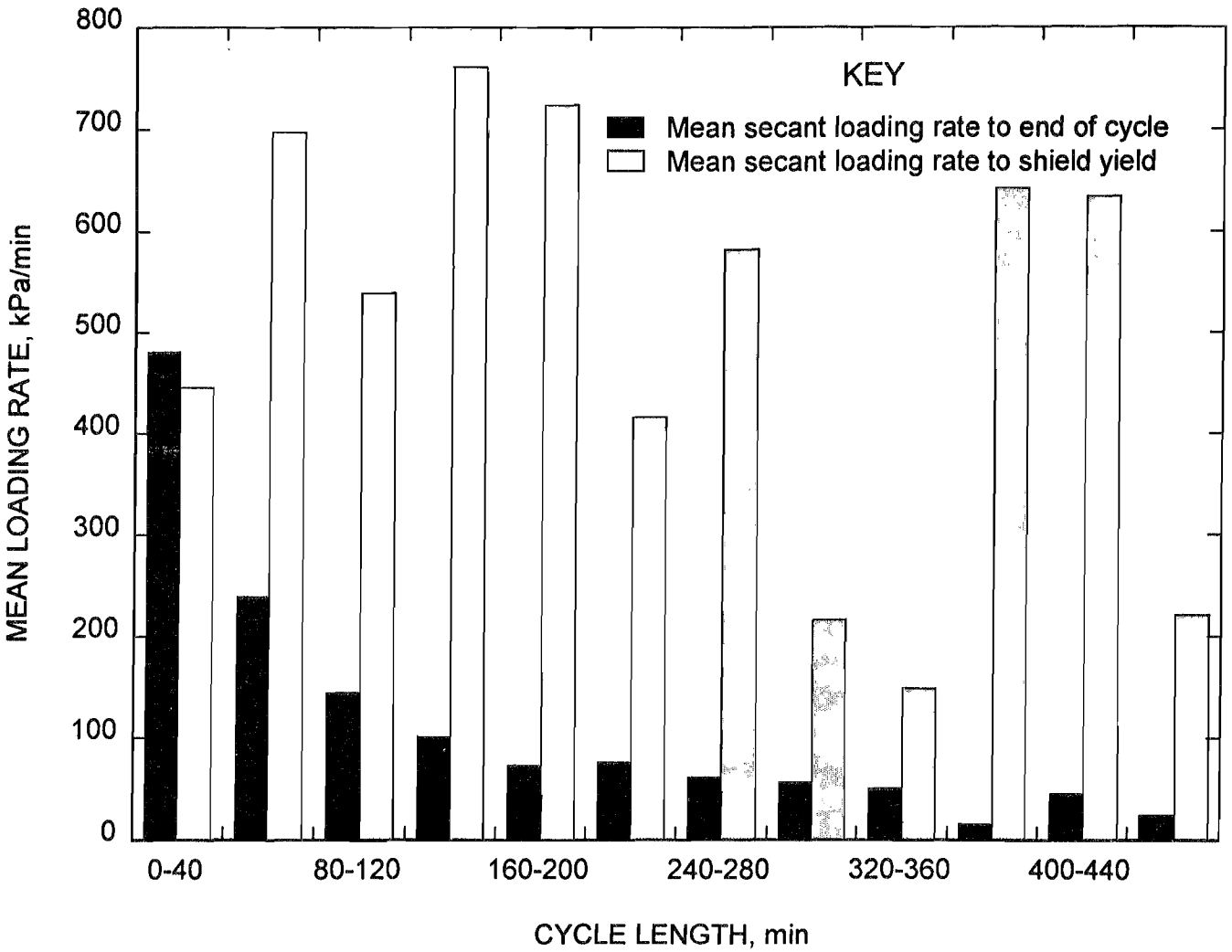

Average secant loading rates versus cycle length. Data are 2,868 yield cycles from the weeks of 1/21, 2/04, 2/11, 2/25, and 3/11/94, grouped by total cycle length.

Figure 14

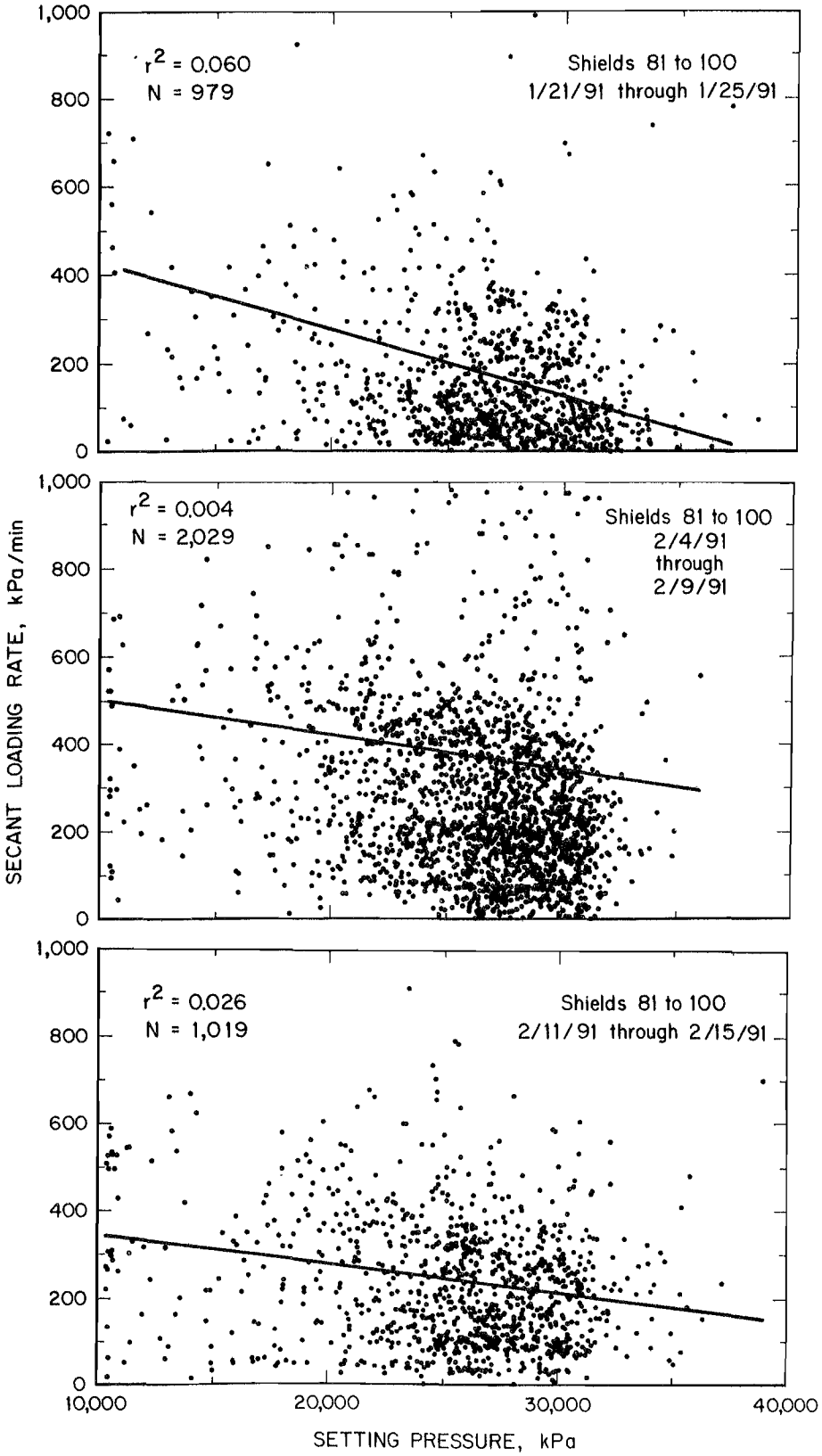

Set pressure versus loading rate. ***N = number of cycles; r^2 = correlation coefficient squared.***

Figure 14—Continued

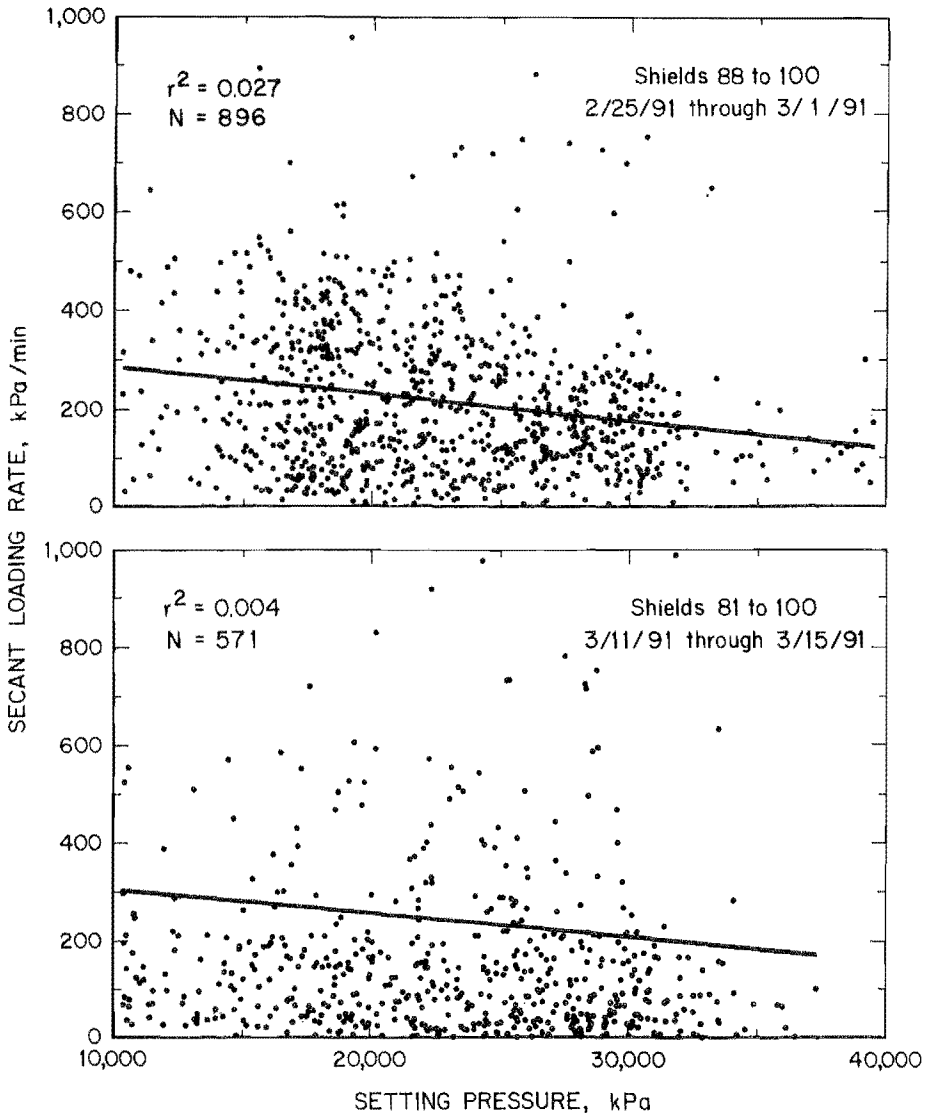

Set pressure versus loading rate. N = number of cycles; r^2 = correlation coefficient squared.

was attempted when the setting pressures of shields 86 to 100 were lowered on February 5 (to a nominal 21,000 kPa) and on February 21 (to a nominal 17,000 kPa). The inconsistency in setting pressures made this test less conclusive, but the results suggest that nonparticipation of shields set at low pressure did not affect shield loading rates. After the setting pressure reductions, the correlation between setting pressures and loading rate remained as low as it had been when setting pressures were at their original values.

A second method of testing the effect of shield nonparticipation was by averaging setting pressure and secant loading rates for a number of shields over a wider portion of the face, and then graphing the averaged setting pressures versus averaged loading rates. The maximum width of face that could be averaged in this study was about 30 m, the distance from shield 81 to shield 100, for periods during which setting pressures had not been reduced. For periods during which setting pressure had been reduced, shields 81 to 85, whose setting pressures were not changed, could not be considered along with the others. For each shearer pass, data from all available legs (cable failures and bad shields forced the rejection of some data for averaging purposes) were used to compute an average loading rate and an average set pressure. The average setting pressure was obtained from the mean of the setting pressures of all legs included in the set. The average loading rate was determined from the mean of the secant loading rates to yield of all included legs. The maximum available number of legs for any cycle was 23 and the minimum number accepted was 6. Of the 296 cycles evaluated, the mean number of legs used in this analysis was 13.4, with a standard deviation of 5.1. The average number of legs included was greatest for the weeks of January 21 and February 4 (14.1 and 16.1, respectively) and lowest for the later weeks (the lowest value was 10.8 for the week of February 25) when data were rejected primarily because of cable failures. The computed data also included an average maximum pressure and cycle length. The averaged setting pressures and loading rates are graphed in figure 15.

The results of the averaged leg data are similar to the results for individual shields. The graph of averaged setting pressure versus secant loading rate (figure 15) shows the same lack of correlation as the graphs for individual legs, and similar regression results were obtained. The r^2 values, also shown in table 2 with the data for individual shields, are again very low and show a low correlation between setting pressure and loading rate. This analysis also suggests that the nonparticipating leg hypothesis is not correct. There is no indication in the data that there is any increase in the average loading rate of the group as average setting pressures for a group of shields decrease.

Observation of the shield pressure curves (for examples, see figures 7 and 12) showed that loading rates decrease with time during most cycles. This effect was then studied in detail by looking at secant loading rates for short portions of each cycle. Computations were made of loading rates in the tailgate side recorder legs (shields 94 to 100) during the weeks of January 21 and February 25. These 2 weeks were chosen to limit the required computations and because they appeared to be representative of conditions before and after the control system changes were made to reduce setting pressures. For every shield cycle during those 2 weeks, the secant loading rates were computed for each 5-min portion of the cycle up to 120 min. Computations were not performed for the end of the cycle after shield yield or when the shearer reached the vicinity of a shield and caused increased loading rates (the shearer effect) through the removal of coal at the face. The loading rates for all shields were then graphed versus leg pressure at the beginning of the interval, and a linear regression was performed on the graph. The graphs are not presented in this report, since they are very similar to those in figure 14, but the equation coefficients and the r^2 values are given in the appendix. The variability of the equation coefficients and the low r^2 values both suggest again that there is no relationship between shield pressure and loading rate during any portion of the cycle up to 120 min.

The secant loading rates for the 5-min periods were then averaged to obtain the mean loading rate for each 5-min interval for all cycles from the weeks of January 21 and February 25. These average loading rates are plotted on figure 16, along with error bars representing ± 1 standard deviation of the averages. Despite the large change in the average setting pressures between those 2 weeks (approximately 4,070 kPa), the curves are quite similar beyond the first 10 min. The shape of the curves suggests that the average shield loading response matches the immediate roof and main roof model described in the "Theory" section of this report. The loading rates at the beginning of a cycle are assumed to be due to immediate roof loading effects, which are highly variable and change from cycle to cycle and from shield to shield. The loading rates during the latter portions of the cycle are assumed to be caused by activity of the main roof, which is more consistent at this site (figure 2). The span of main roof that affects the shields should also be larger, leading to more consistent changes in loading patterns.

Based upon the immediate and main roof model, an equation was chosen to fit the data of figure 16 using an exponential term to fit the early time (immediate roof)

Figure 15

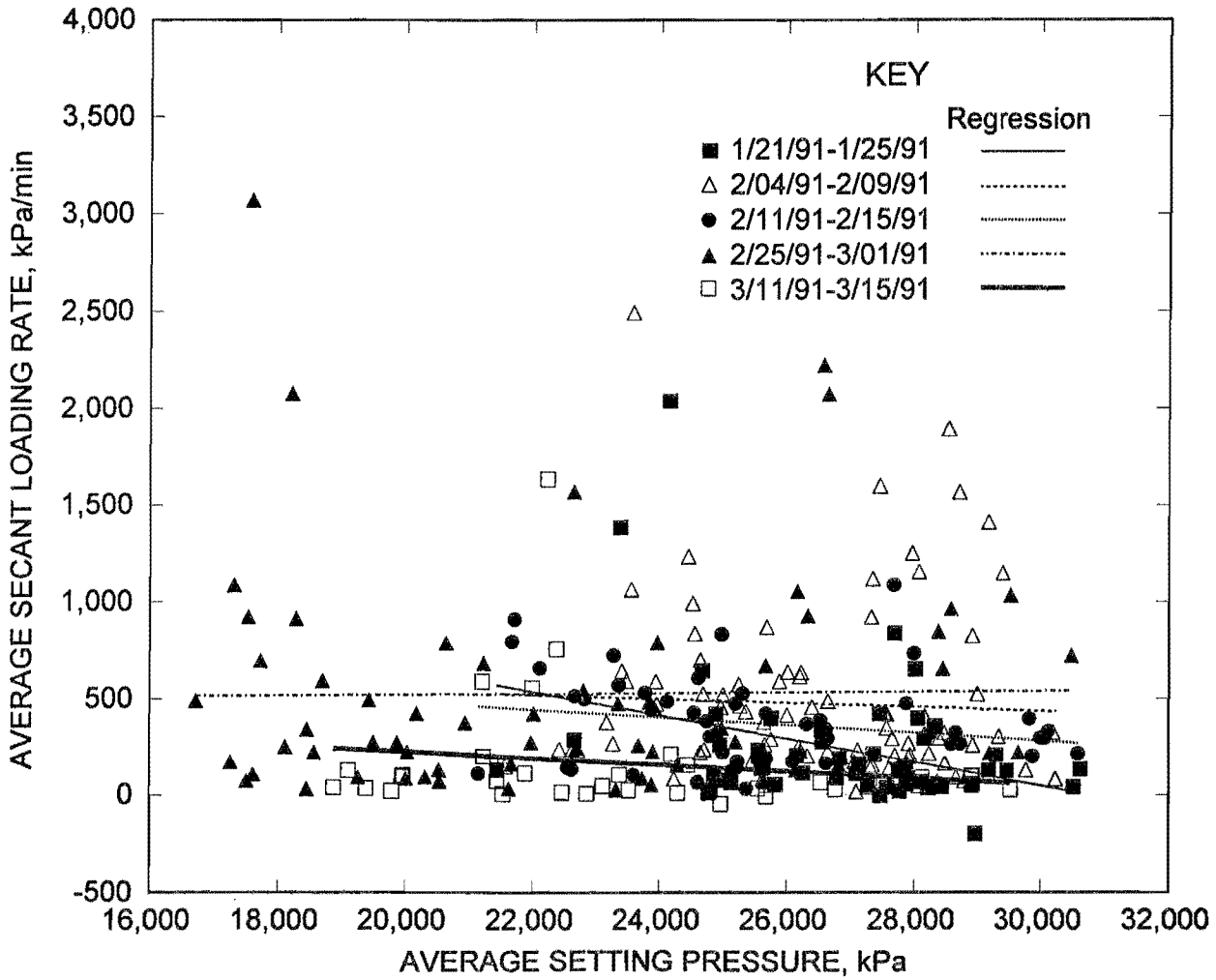

Graph of average set pressure versus average secant loading rate to leg yield.

portion of the cycle and a linear equation to fit the later time (main roof) portion of the cycle. The fitted equations were of the form:

$$R_p = a \cdot e^{bt} + c \cdot t + d,$$

where R_p = leg loading rate, kPa/min,

a, b, c, d = constants of fitted equation,

e = base e constant, e = 2.718281,

and t = time, min.

The r^2 values for the equations were 0.957 (January 21), and 0.990 (February 25). Beyond the first 30 min, the exponential term contributes less than 10 pct of the total value, which matches the assumption of the immediate and main roof theory, that the immediate roof should come to equilibrium. The equations of figure 16 were fitted to averaged data over the range of 0 to 120 min of a shield cycle. If the equations are used beyond a time of 120 min they give obviously erroneous results. The January 21 equation begins to give negative loading rates at times greater than 128 min, and the February 25 equation begins giving negative rates at times greater than 209 min. Observation of weekend shield cycles shows that leg loading can continue after mining stops for at least several days, so

Figure 16

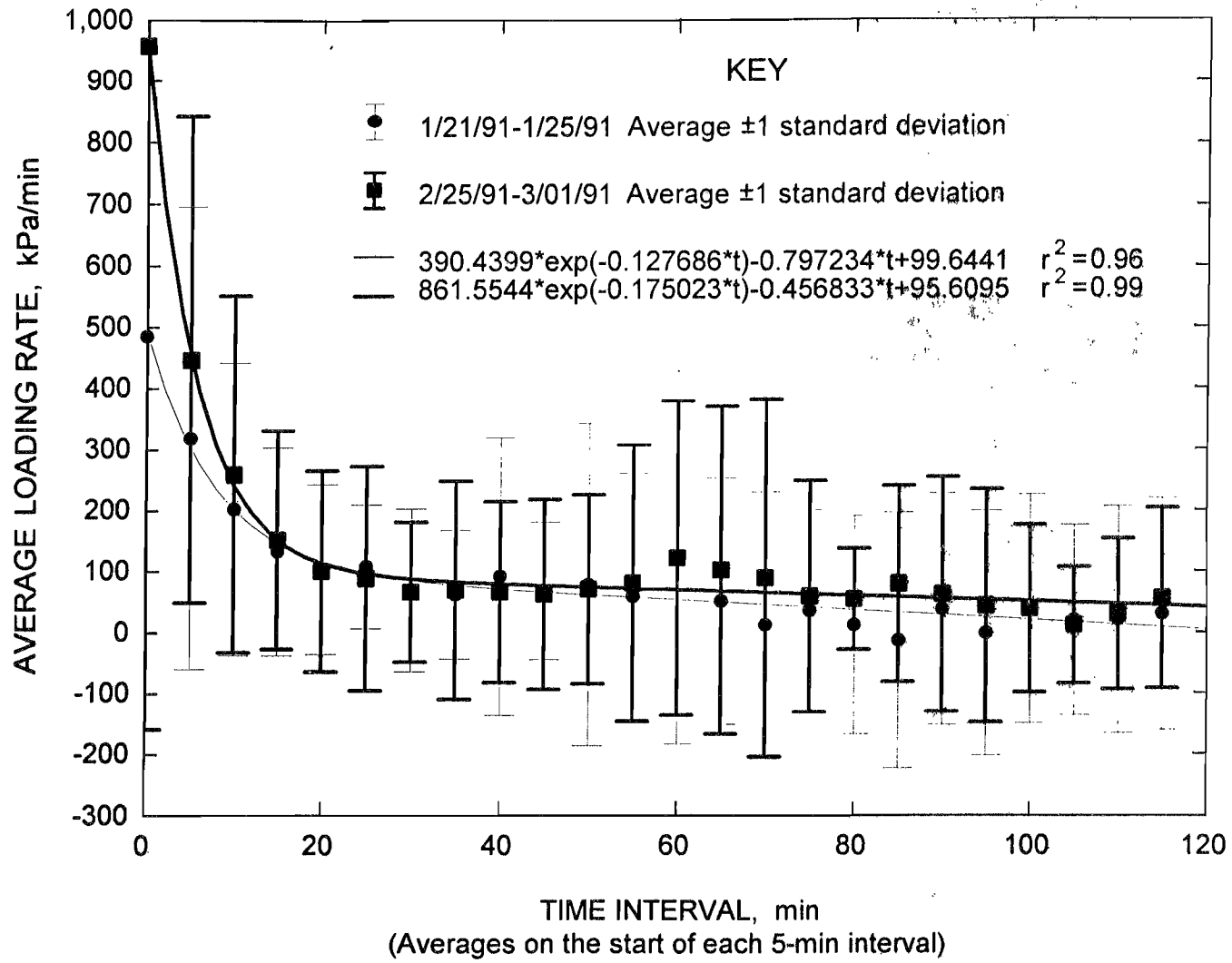

Secant loading rates for 5-min periods versus time, with fitted equations.

the model is obviously not accurate for long shield cycles. The predictive value of these relationships for a single cycle may be appropriately judged by the error bars for each averaged loading rate point on figure 16, although they appear to correlate well with average behavior. The curves may accurately represent the mean loading rate curve, but individual shield cycles typically show much greater variability.

The equations based upon the immediate and main roof model give a good fit to the average shield loading rates for large numbers of cycles. The loading rates for individual cycles are unpredictable, indicating that the equations do not take into account all of the factors controlling shield loading. The roof lithology, possible changes in rock mechanical properties, and joints or fractures are all candidates for explaining the changes in loading rates. However, the geologic data available do not allow testing any of these factors except lithology. The changes in loading rate were found to take place too frequently to be explained by the relatively gradual changes in lithology observed. Loading rates changed drastically several times a day and could vary drastically from cycle to cycle, over distances on the order of 10 m. In contrast, the lithology changed significantly only on the order of 100 m. Data were not available to test the other possibilities, rock mechanical properties and the presence of joints and/or other discontinuities in the rock.

CONCLUSION

Five weeks of shield leg pressure data from the A-2 panel of the Meigs No. 31 Mine were analyzed to determine the effect of setting pressure on shield loading rates. The data were collected over an 11-week period representing 400 m of face advance. None of the data analyzed indicated a correlation between setting pressure and loading rate. This was true when individual shield legs were examined alone and when setting pressures and loading rates were averaged for a number of shields to take into account possible nonparticipating shields.

Shield loading rates were found to be time dependent, with high initial loading rates, which declined during each shield cycle until the shearer again reached the vicinity of the shield. The act of cutting coal near any individual shield then led to increased loading rates in that shield, generally immediately before it was advanced at the end of its cycle. The shield loading rates were modeled by a simple equation that assumed that the behavior of the roof was determined by immediate roof loading, which reached equilibrium in well under 30 min and which was modeled by an exponential term in the equation, and by a constant main roof convergence, modeled as a linear term in the equation. The equations based upon the immediate and main roof model gave a good fit to the average shield loading rates for large numbers of cycles. The loading rates for individual cycles were unpredictable, indicating that factors that were not taken into account are important in predicting loading rates. The rapid changes in loading rates, which could often take place from one cycle to the next, suggest that the unaccounted-for factors include geologic discontinuities that would be difficult to measure and include in any model.

ACKNOWLEDGMENTS

This project could not have been completed without the assistance of the personnel of the Southern Ohio Coal Co. In particular, the author would like to thank Nelson Kidder, engineering superintendent, Steve Doe, senior geologist, and Chuck Bolen, longwall maintenance coordinator, all of whom provided guidance and advice. In addition, the author would like to thank the miners on the A-2 longwall face who went out of their way for months to protect the fragile cables and dataloggers.

REFERENCES

1. Barczak, T. M. The History and Future of Longwall Mining in the United States. USBM IC 9316, 1992, p. 23.

2. Merritt, P. The 1994 Longwall Census. Coal, v. 99, No. 2, Feb. 1994, pp. 26-35.

3. Peng, S. S., and H. S. Chaing. Longwall Mining. Wiley, 1984, pp. 16-21.

4. Barczak, T. M., and D. E. Schwemmer. Stiffness Characteristics of Longwall Shields. USBM RI 9154, 1988, 14 pp.

5. Barczak, T. M., and D. C. Oyler. A Model of Shield-Strata Interaction and Its Implications for Active Shield Setting Requirements. USBM RI 9394, 1991, 13 pp.

6. Zelanko, J. C., G. A. Rowell, and T. M. Barczak. Analysis of Support and Strata Reactions in a Bump-Prone Eastern Kentucky Coal Mine. Paper in Transactions of the Society for Mining, Metallurgy, and Exploration, Inc. (SME Annu. Meet., Denver, CO, Feb. 25-28, 1991). SME, 1991, v. 290, pp. 1894-1900.

APPENDIX.—COEFFICIENTS OF SET PRESSURE VERSUS LOADING RATE REGRESSIONS FOR 5-min SECANT LOADING RATES

Dates	Time interval,[1] min	Intercept, kPa	Slope, kPa/min	Correlation coefficient squared (r^2)
1/21 to 1/25	0- 5	2,559.19472	-0.524960	0.145404
	5- 10	-367.01293	0.158186	0.112928
	10- 15	-190.23551	0.084516	0.101791
	15- 20	-58.40035	0.039540	0.051758
	20- 25	63.08072	0.007972	0.003589
	25- 30	-26.41617	0.025657	0.061868
	30- 35	171.72703	-0.019895	0.024517
	35- 40	28.40399	0.006261	0.004036
	40- 45	139.21572	-0.009151	0.001761
	45- 50	60.82340	0.001191	0.000147
	50- 55	351.59979	-0.050339	0.045125
	55- 60	226.45917	-0.029965	0.025744
	60- 65	447.67931	-0.058163	0.044290
	65- 70	199.47253	-0.026288	0.018462
	70- 75	30.82765	-0.003456	0.000287
	75- 80	68.51856	-0.005895	0.001289
	80- 85	106.11671	-0.015997	0.006776
	85- 90	106.61773	-0.020716	0.010872
	90- 95	222.49634	-0.031013	0.023126
	95-100	166.42698	-0.028458	0.019868
	100-105	167.68358	-0.021984	0.014218
	105-110	151.50132	-0.022740	0.020716
	110-115	128.58388	-0.018560	0.000882
	115-120	387.63817	-0.059784	0.080587
2/25 to 3/01	0- 5	1,702.33750	-0.215068	0.029191
	5- 10	77.40779	0.087881	0.060641
	10- 15	31.20857	0.050049	0.043678
	15- 20	89.86404	0.012826	0.008057
	20- 25	112.84558	-0.002712	0.000450
	25- 30	139.94420	-0.010562	0.005650
	30- 35	106.66609	-0.008200	0.008499
	35- 40	127.35793	-0.011545	0.006970
	40- 45	133.48563	-0.013112	0.012423
	45- 50	96.34682	-0.006647	0.003073
	50- 55	173.63031	-0.019825	0.027329
	55- 60	210.74962	-0.025205	0.020991
	60- 65	233.82174	-0.021377	0.011713
	65- 70	335.54449	-0.043917	0.044634
	70- 75	306.71136	-0.041156	0.032620
	75- 80	238.43799	-0.032090	0.034626
	80- 85	78.41298	-0.004625	0.034626
	85- 90	78.16632	0.000001	0.004676
	90- 95	209.76460	-0.026826	1.59e-10
	95-100	199.64129	-0.027245	0.022112
	100-105	126.09473	-0.159099	0.020120
	105-110	46.82580	-0.006781	0.008783
	110-115	226.59092	-0.034145	0.073691
	115-120	65.98222	-0.001963	0.000268

[1]Portion of cycles for which secant loading rates were computed.

NOTE.—All computations were performed on data from shields 94 to 100, the tailgate side recorder.